Drug Delivery via GLIADEL Wafer for Treatment of Glioblastoma Multiforme (GBM)

William Leif Ericksen, Lyndsey Fortin, Cheryl Hou, Katrina Shum

BEE 453

May 1, 2008

Table of Contents

I. Executive Summary:

Glioblastoma multiforme (GBM), one of the most common primary glial tumors, is often treated with tumor resection surgery combined with GLIADEL wafers containing carmustine. These wafers are made with a degradable polymer that releases carmustine over a period of 5 days. Due to the localized nature of the release, no pharmacokinetic measurements have been taken in humans. In order to study the mass transfer of carmustine, COMSOL Multiphysics was used model the process and solve the transient convection-diffusion problem involved. A 2D axisymmetric geometry was used as a simplified schematic involving the wafer, tumor tissue, and normal tissue regions. Input parameters of diffusivity, reaction rates, and velocities were obtained from research involving carmustine drug delivery in human and monkey tissues. Results obtained showed a large initial increase of drug concentration within the first 12 hours localized within the tumor, followed by an exponential decrease during the remaining time period. This shows that the majority of cellular death was within the tumor. Results also indicated that elimination rate, velocity, and diffusivity were sensitive parameters. Furthermore, the model gave insight into what parameters can be changed in order to increase the concentration of carmustine in the tumor and decrease the concentration in the healthy tissue. Carmustine must be delivered to the tumor tissue at a certain concentration to be effective, so optimizing the parameters involved would create a better drug delivery system.

Key words: drug delivery, glioblastoma multiforme, carmustine

II. Introduction and Design Objectives

II.i Background and Importance

Glioblastoma multiforme (GBM) is the most common of all primary glial tumors. Despite advances in diagnostic imaging and drug discovery, primary malignant brain tumors remain fatal. The treatment of GBM is merely palliative and includes surgery, radiotherapy, and chemotherapy; however, the median survival rate with treatment is a mere 8 months. The most difficult challenge in treating brain tumors is the impenetrability of the blood-brain barrier (BBB), as chemotherapy treatments taken orally or intravenously do not diffuse into the brain effectively or efficiently. However, local delivery of chemotherapy to brain tumors has provided a way to circumvent the blood-brain barrier, allowing delivery of chemotherapy drugs directly to the malignant brain cells.

One method of local delivery that has been developed is polymeric-controlled release. One type of degradable polymer which has been used in the post operative treatment of GBM is the GLIADEL® wafer. These dime-sized wafers are 14 mm in diameter and 1 mm thick, loaded with 7.7 mg of the chemotherapy drug carmustine. Up to eight wafers are implanted along the walls and floor of the resulting cavity after surgical resection of a GBM tumor. The wafers degrade slowly, delivering carmustine to the surrounding cells, preventing the aggressive GBM tumor from reoccurring.

Studies have been done in both rodent and non-human primate brains at various times after implantation to investigate the effectiveness of the GLIADEL wafer. These studies have shown the capability of the GLIADEL® wafer to produce high dose-delivery within millimeters of the polymer implant, with a limited penetration distance. However, due to the localized nature of the drug in the brain tissue, no direct pharmacokinetic measurements have been made in humans after the implantation. For our project, we modeled drug delivery from a GLIADEL® wafer to the surrounding tissue in a surgical resection site in order to investigate human pharmacokinetic properties.

Additionally, animal studies have presented conflicting results as to whether or not convection in the interstitial fluid has a significant effect on the delivery of carmustine. By running our model with and without convection, we will investigate whether or not it has a significant effect on our results.

II.ii Problem Schematic

Figure 1 shows the 3D geometry of our model. As surgeons cannot resect an entire GBM tumor without damaging healthy tissue, a minimal layer of tumor remains in the cavity. Therefore, our model depicts the wafer placed on a small layer of tumor tissue, as opposed to healthy tissue. Diffusion from the sides of the wafer is assumed to be zero as the wafer is much wider than it is thick.

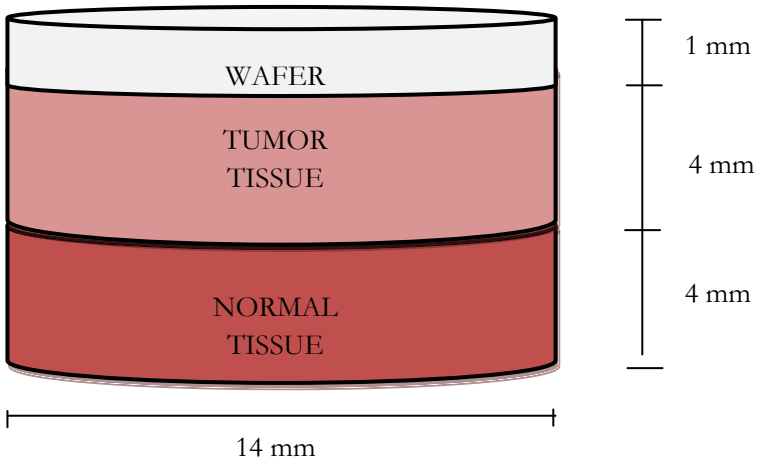

Figure 1: Geometry of Problem. The wafer is placed in the tumor resection cavity atop of the residual tumor tissue. Once the drug has diffused through the tumor tissue, it will reach the healthy tissue.

In order to reduce computation, the schematic shown in Figure 2 was used in our model.

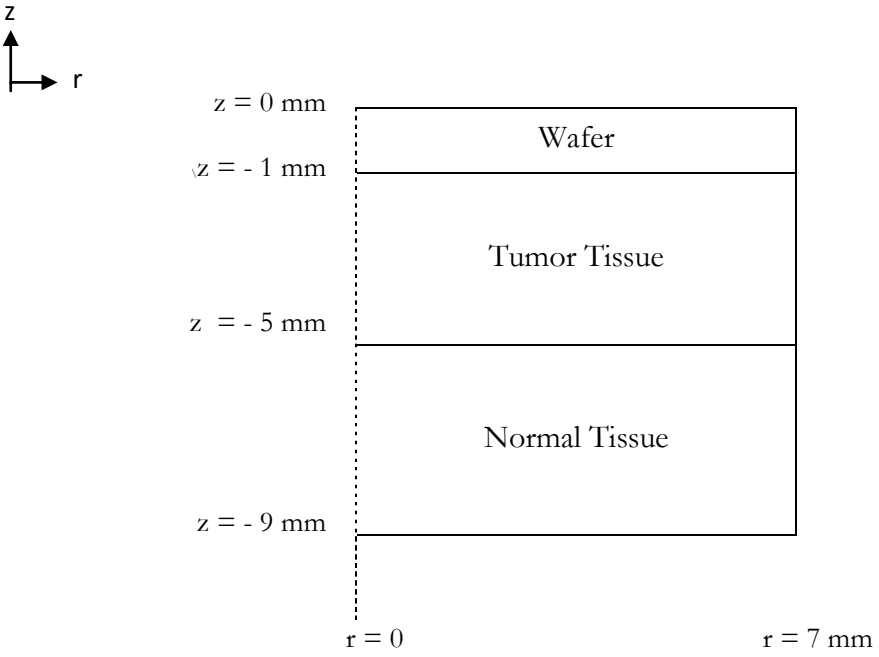

Figure 2: Problem Schematic. A 2D axisymmetric geometry was used, with the dotted lines representing the axis of symmetry. The flux at the top of the wafer was assumed to be zero as there is no tissue for the drug to diffuse into. The flux on the sides is zero because we assumed the drug is only diffusing in the vertical direction. The flux at the bottom of the tissue layer is zero because it is assumed semi-infite.

The boundary conditions, as well as initial conditions, are also explained in Appendix A.

II.iii Design Objectives

We modeled the delivery of carmustine from a Gliadel wafer into the human brain in order to study the effects of diffusion, convection, and elimination of the drug carmustine. As *in vivo* studies have shown that carmustine release occurs over a period of approximately 5 days, we performed our study over this time period. In response to conflicting research, we investigated the significance of convection in carmustine drug delivery. Additionally, we determined which parameters are most sensitive in the drug delivery process in order to gain insight into which parameters might be altered to produce an ideal concentration profile. Ideally, the carmustine will be delivered in high concentrations to the tumor tissue while minimizing concentrations in the healthy tissue, which could cause damage to brain.

III. Results and Discussion

Our first simulation was run without convection. The input parameters for diffusivity and elimination used are found in Table A2. The initial concentration used for the wafer is found in Table A1.

In our second simulation, a convection value of 3.23×10^{-11} m/s was applied to the normal tissue region. The convection-time plots at the tumor-normal tissue interface (at 5 mm depth) for the two simulations were compared, as shown in Figure 3.

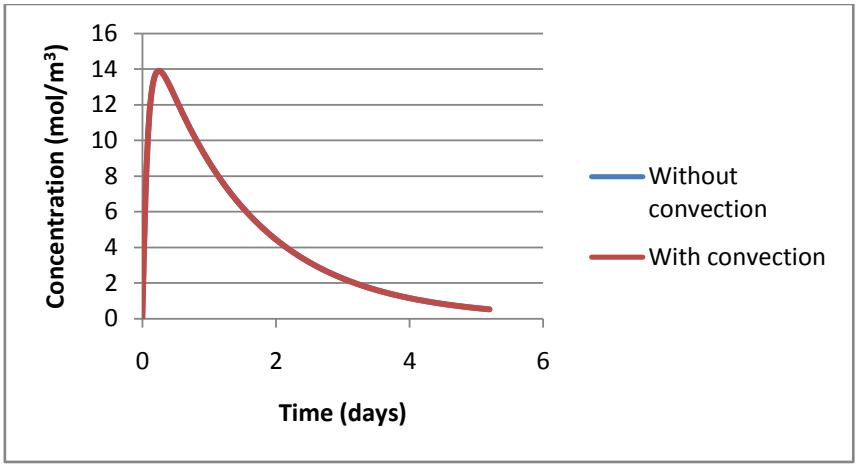

Figure 3: Time concentration profile at the tumor-normal tissue interface with and without convection.

The overlap of the two curves shows that convection does not significantly affect our results. Therefore, the rest of our simulation was performed with a convection value of 3.23×10^{-11} m/s in the normal tissue region. This would allow our model to better represent the real-life situation of fluid movement present in the resection cavity after tumor resection.

The surface plot of our results for our entire schematic is shown in Figure 4. As can be seen, there is a drastic change in color between the wafer and tissue sections of our model, which shows that the concentration of carmustine in the wafer is a lot higher than the concentration in the tumor and normal tissue.

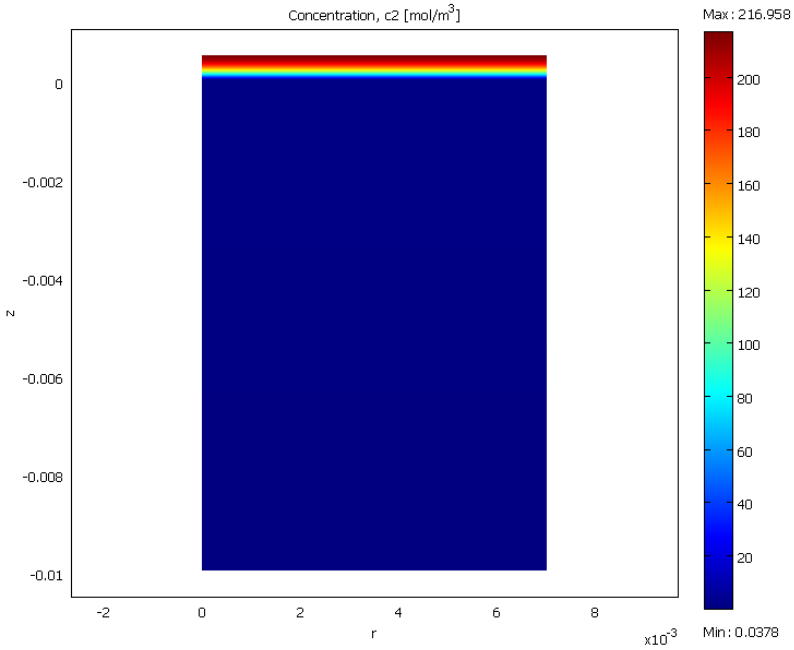

Figure 4: Surface plot for concentration of the wafer, tumor and tissue at 5 days.

This contrast is better visualized by the line-plot as shown in Figure 5. There is a steep drop in concentration from around 220 mol/m^3 to less than 2 mol/m^3 from the wafer to the tissue. This almost 100-fold difference is significant because it indicates a large partition coefficient between the wafer and the tissue. This should be taken into consideration when designing our wafer.

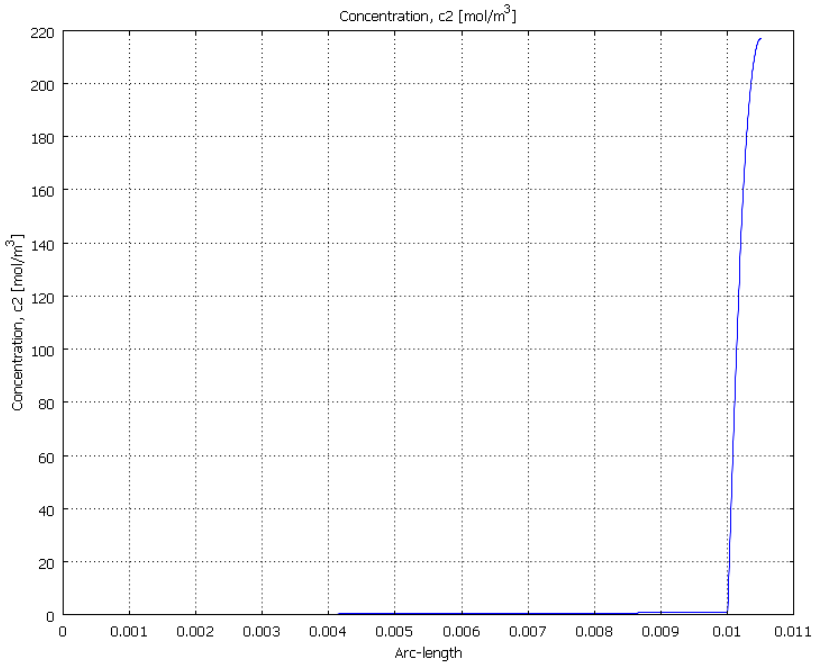

Figure 5: Line plot for concentration of the wafer, tumor and tissue at 5 days.

The difference in concentration within the tumor and normal tissue regions (without the wafer) are better visualized in the surface and line plots in Figures 6 and 7, respectively. As can be seen from the color gradient in the surface plot, there is a steady decline in concentration from the tumor-wafer surface into the normal tissue. The highest concentration found in the tumor tissue is 0.877 mol/m^3, while the smallest concentration found in the normal tissue is 0.0378 mol/m^3.

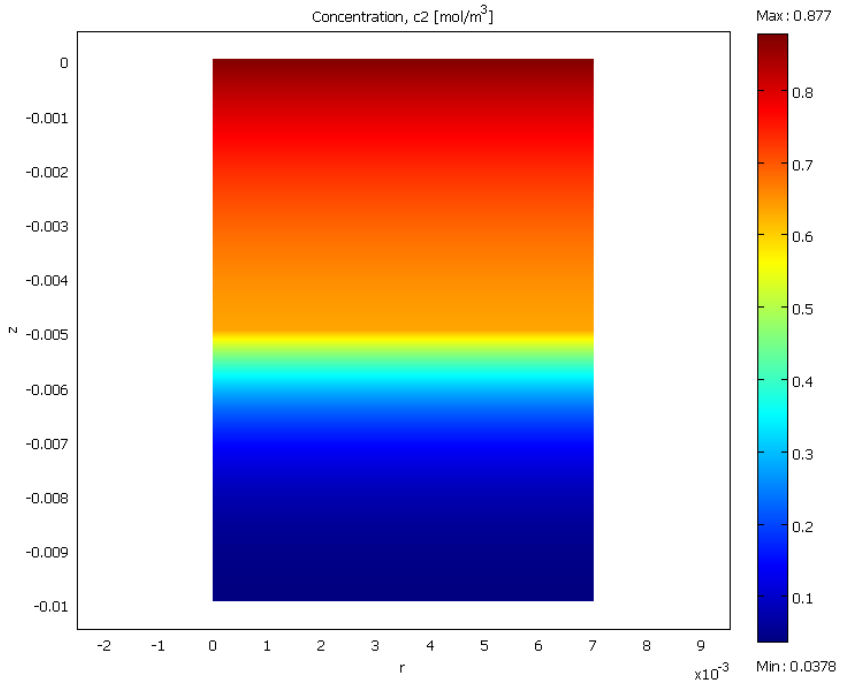

Figure 6: Surface plot for concentration of the tumor and tissue at 5 days.

As can be seen from the line plot (Figure 7), there is a steady decline in concentration until the 5-mm point, where the slope of the decline suddenly increases. The concentration rapidly drops at the top portion of the normal tissue until it begins to level out again at 7-mm depth of tissue. This means that the higher concentration of carmustine remains in the tumor portion of the model. This result is favorable, because a higher concentration of drug in that region will kill the tumor tissue, with minimal damage to the normal tissue.

Our results are comparable to the results of Saltzman and Fleming, gathered from the monkey brain, because they also observed a decline in drug concentration from the polymer-tissue interface. Their measured values, however, do not show a sharp decline in concentration that we observed at the 5-mm point. This may be due to the lack of a clear boundary between tumor and normal tissue that occurs in real-life, in contrast to our model, which specified a definite change in tissue diffusivities between the tumor-normal tissue interface.

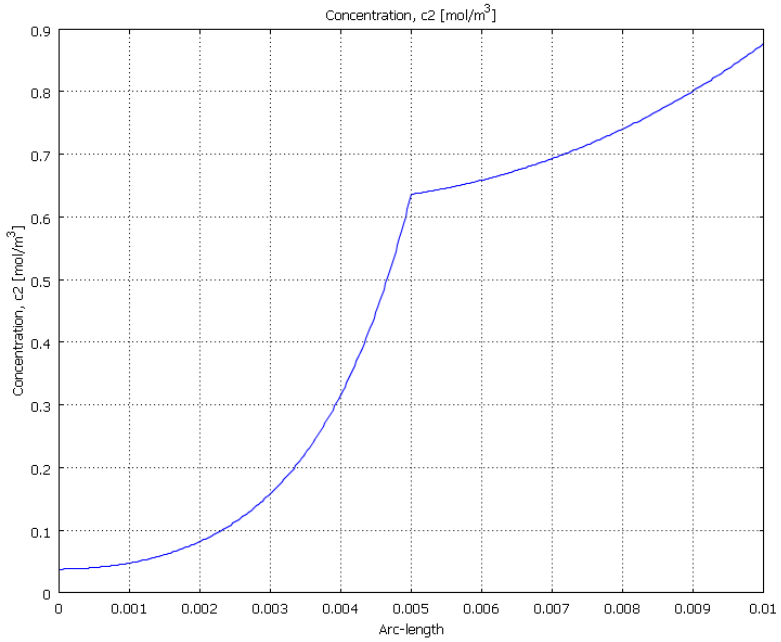

Figure 7: Line plot for concentration of the tumor and tissue at 5 days.

The time concentration plot of our results at the 5mm point, as shown in Figure 3, shows that the highest concentrations at the tumor-normal tissue interface is reached at half a day. After this point, there is an exponential decline in concentration until day 5. This is consistent with the results obtained by Saltzman and Fleming, where their highest concentration values were obtained within the first day. This result is significant because this way, we can monitor the highest concentration values that are reached for various parts of our tissue and determine whether significant peak concentration values were reached in order to kill the tissue. We can also determine whether the time period during which these peak concentration values were reached is long enough for tissue degradation.

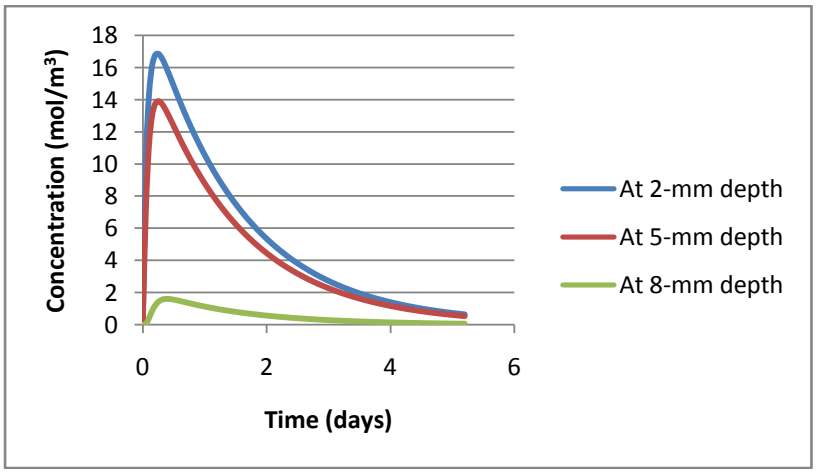

Figure 8: Time concentration profile at various depths with convection.

The line plot for our results at various time points is shown in Figure 9. As can be seen, the highest concentration value reached in the tumor tissue at half a day is about 17.5 mol/m^3. Additionally, the

concentration value at 1-mm depth at 1 and 3 days are about 11 mol/m^3 and 3 mol/m^3, respectively. This is comparable to the Saltzman and Fleming values of 1.5 mol/m^3 and 0.3 mol/m^3.

The significant difference between our results and experimental results may be contributed to the fact that we are comparing human values with experimental monkey values. In addition, there are no human pharmacokinetic values for carmustine due to the localized nature of the drug. We had to use human values obtained from simulation as well. Our sensitivity analysis also shows that elimination rate has a significant influence on our results; thus, a small difference in elimination rate may produce a significant difference in our results.

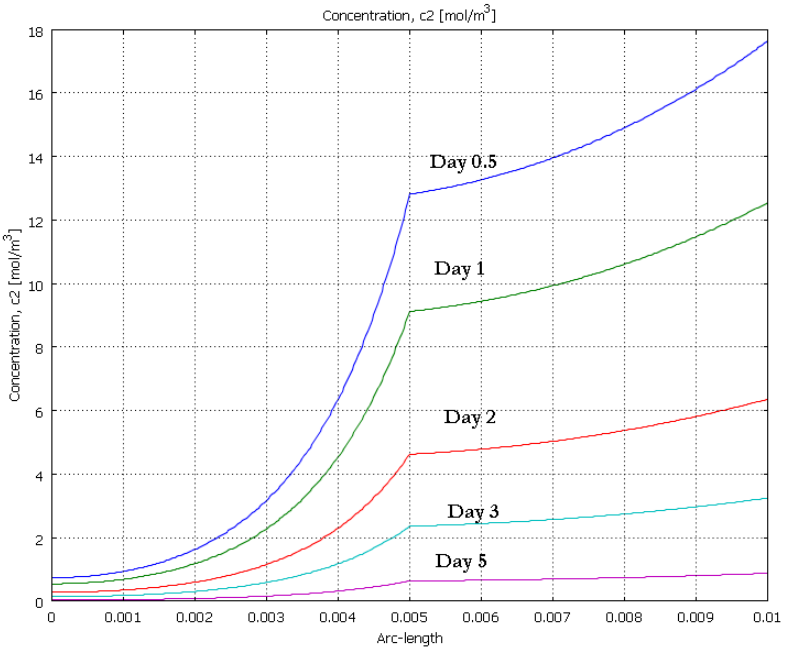

Figure 9: Line plot for concentration of the tumor and tissue at 0.5, 1, 2, 3, and 5 days.

III.i Sensitivity Analysis

Velocity:

We performed a sensitivity analysis on velocity in order to measure the effects of velocity on our results. Figure 10 shows our results for average concentration in the tumor and normal tissue at various velocity values. Our analysis showed that the velocity (pressure change) has a much more significant effect on concentration changes when the velocity was increased to a magnitude of 10^{-7}. Figure 11 displays the results of our time-concentration plots at varying velocities. These graphs show a significant decrease in concentration at the tumor and tissue interface (5 mm depth) as velocity increases. The lower concentration can be due to the higher convection influences that take away the drug. This results in a lower average concentration of drug in the tumor and a higher average concentration of drug in the tissue.

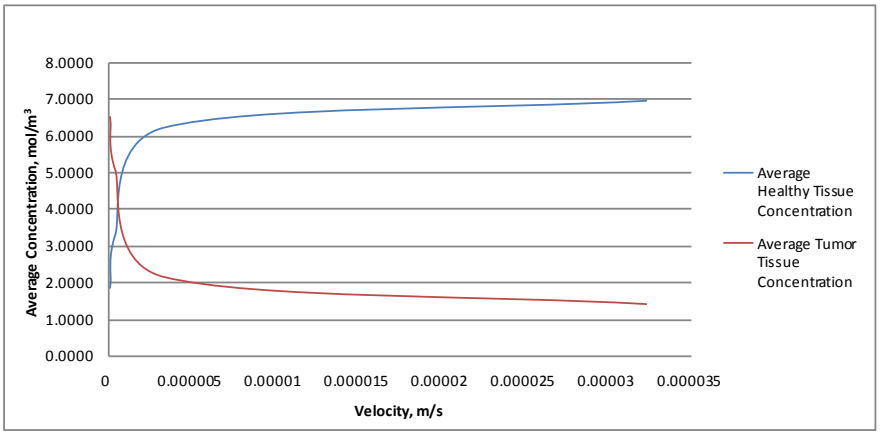

Figure 10: Plot of average drug concentrations in the tissue and the tumor for varying velocity values.

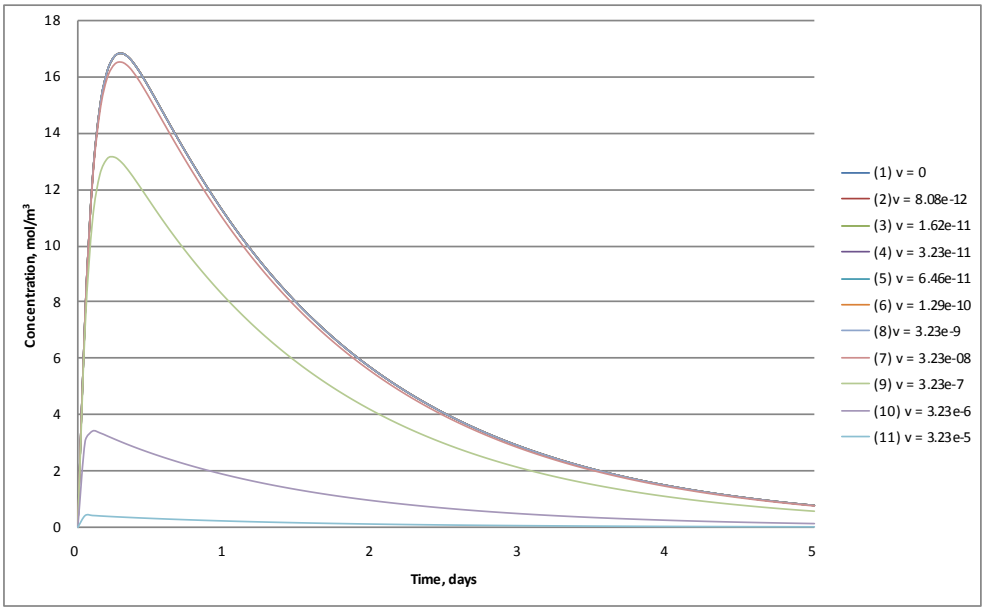

Figure 11: Time concentration plots for different velocity values at 5mm depth.

Elimination Rate:

Figures 12 and 13 show our sensitivity analysis results for the elimination rate. Our analysis shows that elimination does have a significant effect on the results. As elimination rate increases, more drug is removed, thus decreasing the concentration of drug. A 10-fold decrease in elimination rate increases the average concentration of drug by about 10 times in the tumor and by more than 20 times in the normal tissue. A 10-fold increase in elimination rate decreases the average concentration of drug by about 8 times in the tumor and 50 times in the normal tissue (Figure 12). The concentration profile is also changed with only a doubling or halving of the elimination rate (Figure 13). This shows that the choice of elimination rate to use for modeling is important for accurate solutions.

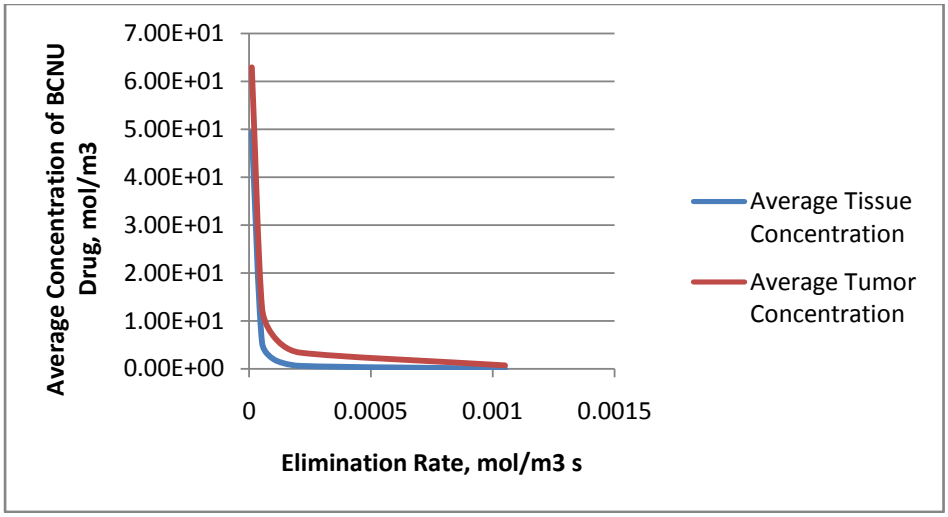

Figure 12: Plot of average drug concentrations in the tissue and the tumor for varying elimination rate values.

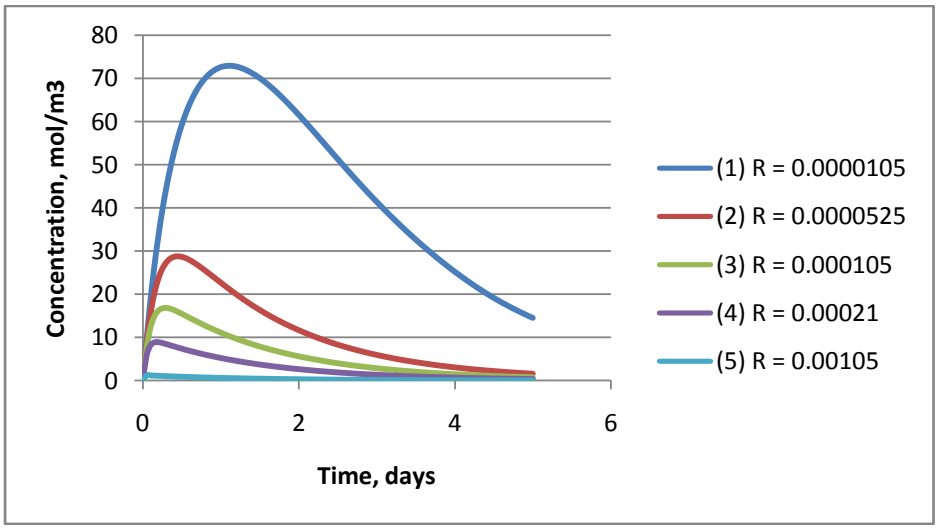

Figure 13: Time concentration plots for different elimination rate values at 5mm depth.

Diffusivity:

Figure 14 below depicts the effect of diffusivity on the concentration profiles. Table 1 lists the diffusivities used in the various data sets in Figure 14. Although the different combinations of diffusivities have been varied, there is a general trend. As the both diffusivities are decreased the peak concentrations decrease, and as both diffusivities increase, the peak concentration increases. Figure 15 clearly shows the smaller concentration profiles with smaller diffusivities and larger concentration profiles with higher diffusivity values. What is unusual is that the middle values of diffusivities had the highest peak concentrations, while the higher diffusivities had the next highest peak concentrations, followed by the smallest diffusivities.

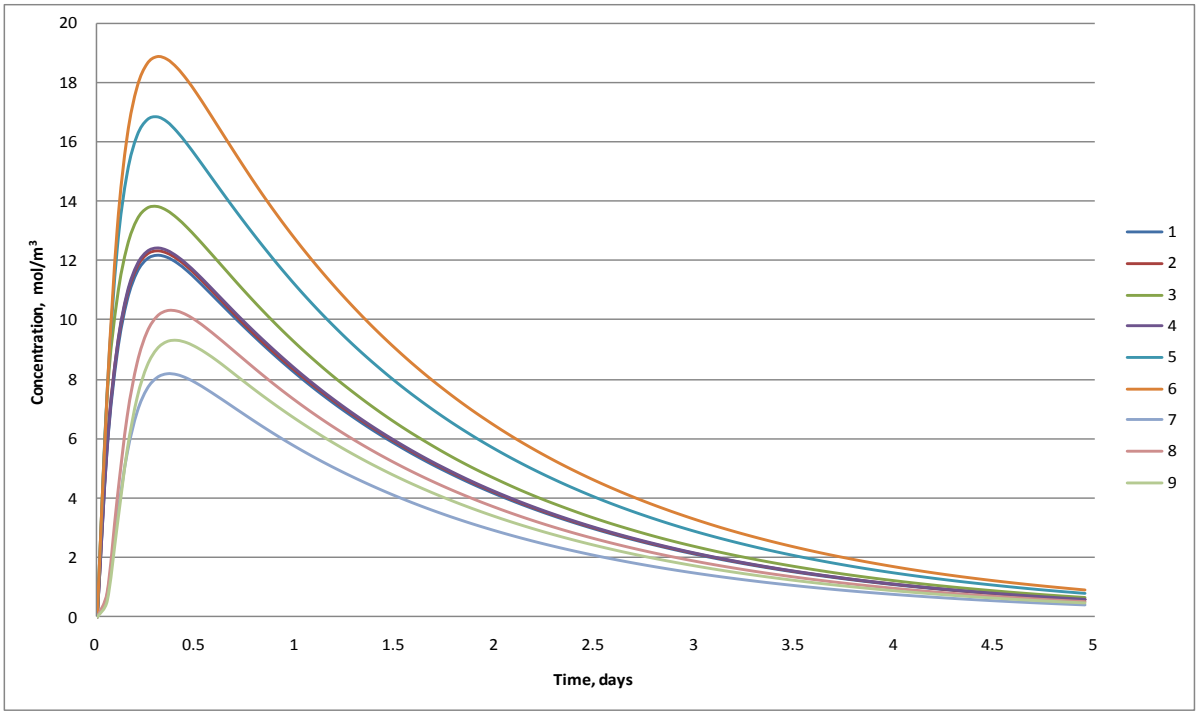

Figure 14: Diffusivity Sensitivity Analysis

Data Set	Diffusivity, m^2/s	
	Tumor	Healthy
1	6.75×10^{-7}	2.5×10^{-8}
2	6.75×10^{-8}	2.5×10^{-8}
3	6.75×10^{-8}	2.5×10^{-9}
4	6.75×10^{-9}	2.5×10^{-9}
5	6.75×10^{-9}	2.5×10^{-10}
6	6.75×10^{-9}	2.5×10^{-11}
7	6.75×10^{-10}	2.5×10^{-10}
8	6.75×10^{-10}	2.5×10^{-11}
9	6.75×10^{-10}	2.5×10^{-12}

Table 1 : Varied Diffusivity Values for the Tumor and Healthy Tissue

Initial Concentration of Carmustine:

Figures 15 and 16 show the sensitivity analysis of the initial concentration in the wafer. Figure 15 illustrates how the initial wafer concentration affects the 2 day average concentration in the tumor or healthy tissue. Once the initial concentration of the wafer is over approximately 120 mol/m^3, the average concentration in the healthy and tumor tissue level off indicating less sensitivity over that initial wafer concentration (Figure 16.) The overlapping concentration profiles in Figure 16 demonstrate that the concentration at the tumor-healthy tissue interface is not really affected by varying the initial concentration of the wafer.

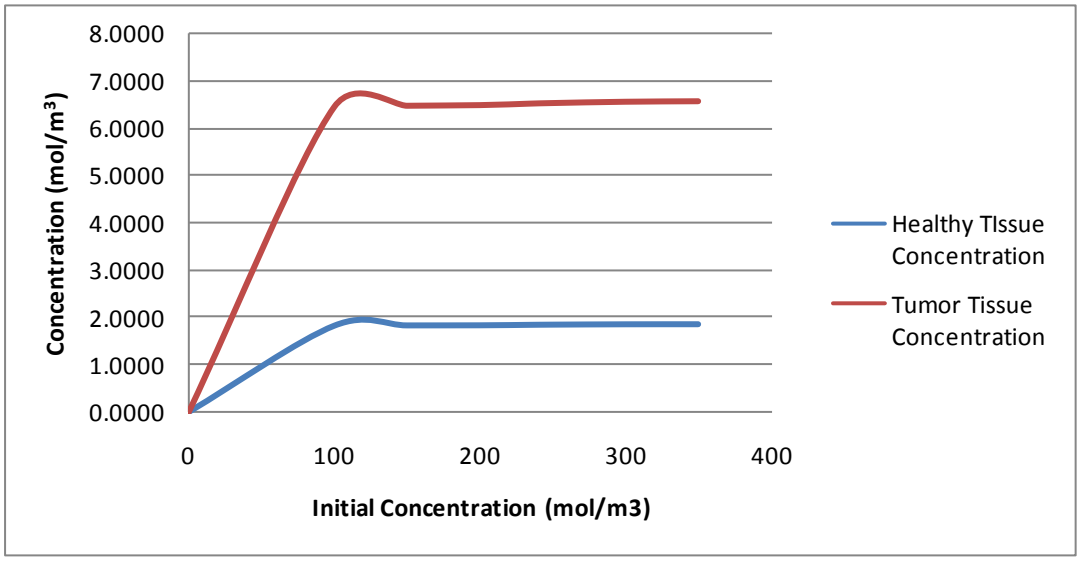

Figure 15: Sensitivity Analysis Initial Concentration of Wafer

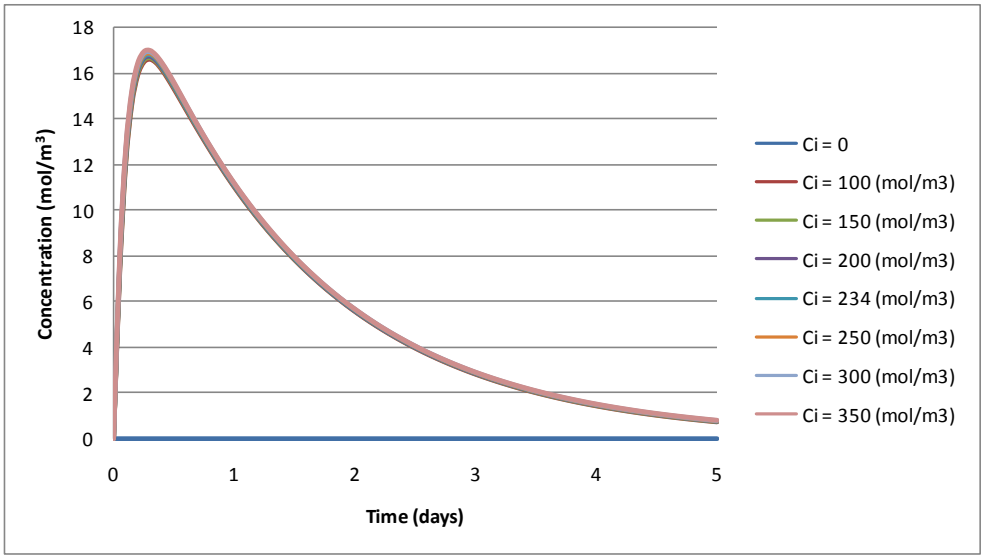

Figure 16: Time-Concentration Plot at the Tumor-Healthy Tissue Interface When Varying Initial Wafer Concentration

IV. Conclusions and Design Recommendations

IV.i Conclusions

Using COMSOL, we successfully modeled the delivery of carmustine from a GLIADEL wafer to the surrounding tissue in a GBM tumor resection cavity over a period of 5 days. The two modes of mass transfer, convection and diffusion, were included in our model along with an elimination source term. Results indicated that carmustine was delivered at high concentrations within the residual tumor tissue, with minimal drug diffusion into the healthy tissue. Concentration values were similar to results found in animal studies, being the same order of magnitude.

In addition, peak concentrations were reached within 12 hours, and declined exponentially soon afterwards. Peak concentrations were found to be 20 and 3 mol/m^3 in the tumor and healthy tissue, respectively. Furthermore, using parameter values from a study by Wang (1999), convection was found to be insignificant in the drug delivery of carmustine.

The sensitivity of four parameters was investigated: convection velocity, rate of elimination, diffusivity, and initial concentration. Convection velocity effects were found to be significant only at interstitial bulk fluid velocities above 10^{-7} m/s. Rate of elimination was found to be extremely sensitive; increasing or decreasing the rate of elimination by just one order of magnitude dramatically changed the resulting concentration-time profile. However, variation in initial concentration of carmustine showed to have an insignificant effect on the concentration-time profile. Finally, diffusivity was found to have a significant effect on the concentration profile. Results indicated that our diffusivities seemed to have an optimal value, because higher diffusivities had higher concentration profiles than the small diffusivities but lower than the middle diffusivity values.

IV.ii Design Recommendations

By performing a sensitivity analysis on the relevant parameters of our controlled-release polymer, we were able to gain insight into which of those parameters should be varied in order to produce the ideal concentration profile. The ideal concentration profile has a high concentration of carmustine in the tumor region, and a low concentration in the healthy tissue region.

In order to get a greater penetration depth of carmustine, the easiest parameters to vary are the rate of elimination and the diffusivity. If the polymer wafer was made of a more porous material, the diffusivity within the wafer would increase and the concentration within the tumor would increase without necessarily increasing the concentration in the healthy tissue by a significant amount. In order to increase the diffusivity of carmustine within the tissue, the structure itself may need to be reformulated. To increase diffusivity the effective diameter should be decreased by either adding functional groups to decrease the solubility or irrigating the cavity with a liquid that has a lower viscosity.

Alternatively, the rate of elimination of carmustine could be lowered. This modification could be made by adding functional groups that block the alkylation site. This would decrease the rate of decay, and therefore increase the penetration depth.

IV.iii Realistic Constraints:

Economic:

Drugs take a LONG time and a LOT of money to be developed, tested and approved by the FDA. Recently, the Supreme Court ruled that customers can no longer sue drug manufacturers, only the FDA, so scrutiny will increase sharply. Therefore, if the structure of carmustine is to be altered to increase diffusivity or decrease the rate of elimination, that should be done immediately because it will take the most time.

Health and Safety:

Though minimal damage to healthy tissue is ideal, eliminating all of the cancerous tissue is paramount. Trying to reduce the amount of carmustine inserted as suggested in design recommendations, therefore, may not be the wisest gamble.

V. Appendix A: Mathematical Statement of the Problem

Geometry and Schematic

Included in *II.ii.*

Governing Equation

The governing equation used for this analysis was as follows:

$$\frac{dc_a}{dt} + u\frac{dc_a}{dz} = D_a\frac{d^2c_a}{dz^2} - k_a c$$

Where u is the velocity defined by the equation, $u = -k\nabla P$ (where k is the interstitium hydraulic conductivity), D_a is the diffusivity in the tumor or normal tissue, and k_a is the first order reaction rate in the tissue. All the terms were used considering this is a transient problem with bulk fluid flow in normal tissue. Carmustine is being used up in both tissue types which is represented by the first order reaction rate.

Initial and Boundary Conditions:

Assuming that there is no drug transport from the sides of the tissues, there is an insulated boundary condition at both sides. We will assume that the concentration of tissue does not reach the end of the normal tissue, so an insulated boundary condition was applied there as well. Each axis of symmetry also have insulated boundary conditions given the symmetry of the problem. Between the wafer and the tumor tissue, a flux is defined as $F = F_o e^{-t/\tau}$ where F_o and τ are constants. This boundary condition was found in a paper describing the delivery of carmustine to brain tumors (Wang, 1999). The boundary between the tumor tissue and normal tissue is a continuity boundary.

The wafer was assumed to have given initial concentration of 233.7 mol/m^3. The tissues did not have any initial concentration.

All the constants used in each boundary and initial condition are can be seen in Table A.1.

Boundary Conditions	Initial Conditions
$-D_a \left.\frac{dc_a}{dr}\right\|_{r=0mm} = 0$	$c_{a,wafer}(t = 0\ s) = 233 \frac{mol}{m^3}$ [2]
$-D_a \left.\frac{dc_a}{dr}\right\|_{r=7mm} = 0$	
$-D_a \left.\frac{dc_a}{dz}\right\|_{z=0mm} = 0$	
$-D_a \left.\frac{dc_a}{dz}\right\|_{z=-9mm} = 0$	
$-D_a \left.\frac{dc_a}{dz}\right\|_{z=-1\ mm} = \left(1.57 \times 10^{-5} \frac{mol}{m,^2 s}\right) e^{-t/(1.26 \times 10^5 s)}$ [4]	

Table A.1: Summary of Boundary and Initial Conditions

Input Parameters

The input parameters are summarized in Table A.2

Property	Region		
	Wafer	**Tumor Tissue**	**Normal Tissue**
Diffusivity, m^2/s	6.7 x 10^{-14} [1]	6.75 x 10^{-9} [4]	2.5 x 10^{-10} [4]
Velocity, m/s	0	0	-3.23 x 10^{-11} [4]
Reaction rate, mol/m^3 s	0	1.31 x 10^{-4} [4]	1.31 x 10^{-4} [4]

Table A.2: Summary of Input Paramters

VI. Appendix B: Mesh & Mesh Convergence

To analyze carmustine delivery from a polymer wafer into the tumor and normal tissue, a software, COMSOL Multiphysics, was used. COMSOL analyzed the transient convection diffusion equation discussed in Appendix A. Our time step was every 4320 seconds for a total of 5 days (432000 seconds.) Calculations were performed with a 0.01 relative tolerance, and a 0.0010 absolute tolerance.

Mesh

Our geometry allowed use to use mapped mesh parameters. This is seen in the below figure.

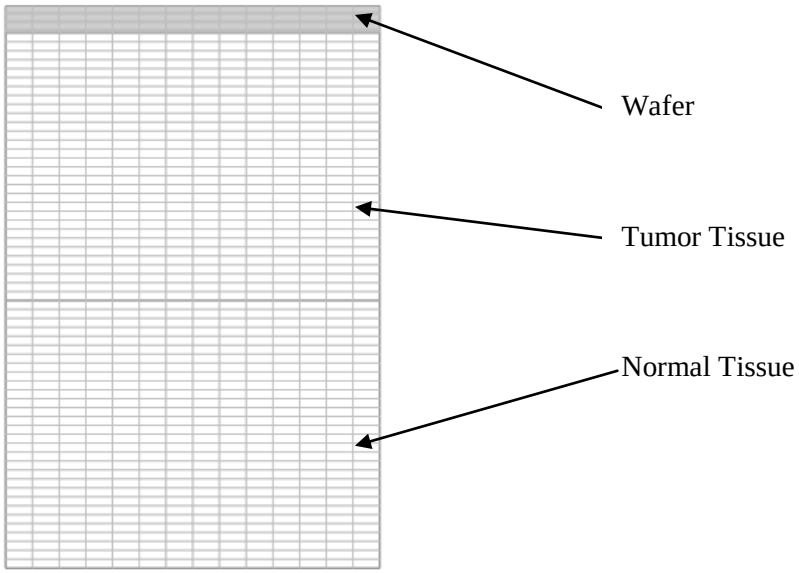

Figure B.1: Mesh Plot for Overall Schematic

A mesh convergence analysis was performed to make sure that the number of elements did not affect the solution. As seen in Figure B.2, between the range of 350 and 1400 elements, there was not much variation between the total concentration in the tumor tissue or normal tissue. We can therefore conclude that the mesh has converged and is not a factor affecting our results.

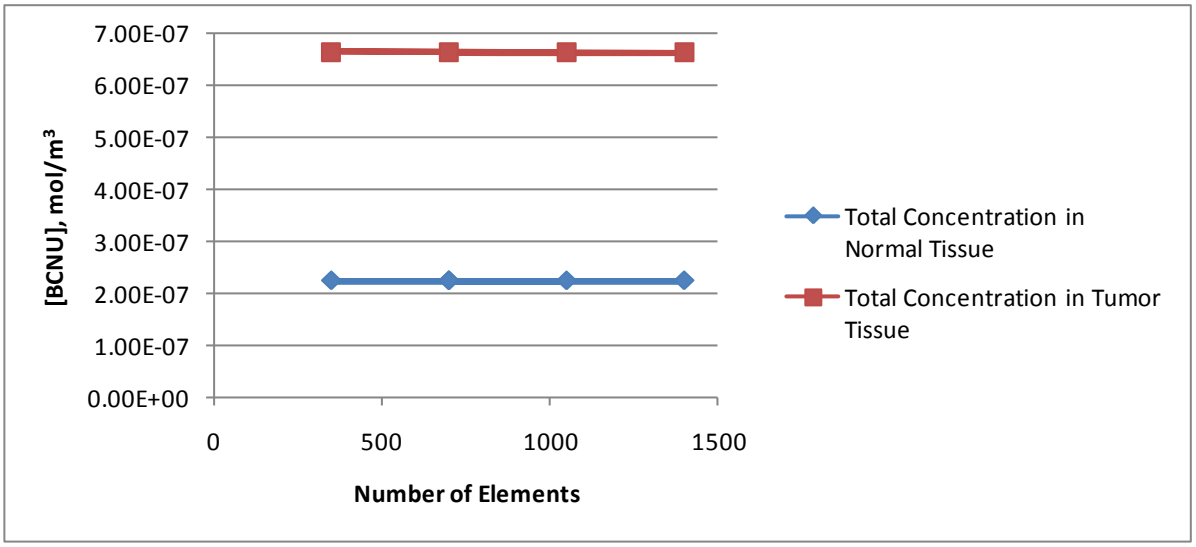

Figure B.2: Mesh Convergence Analysis at 5 days

Appendix C: References

1. Fung, Lawrence, et al. *Pharmacokinetics of Interstitial Delivery of Carmustine, 4-Hydroperoxycyclophosphamide, and Paclitaxel from a Biodegradable Polymer Implant in the Monkey Brain*. Cancer Research. 58 (1998), 672-684.
2. Fleming, Alison, and W. Mark Saltzman. *Pharmacokinetics of the Carmustine Implant*. Clinical Pharmacokientics. 41:6 (2002), 403-419.
3. Kauppinen, Risto A. *Monitoring Cytotoxic Tumor Treatment Response by Diffusion Magnetic Resonance Imaging and Proton Spectroscopy*. NMR in Biomedicine. (2001.)
4. Wang, Chi-Hwa, Li, Jian, Teo, Chee Seng, and Timothy Lee. *The delivery of BCNU to Brain Tumors*. Journal of Controlled Release. 61 (1999), 21-41.